



Supplementary Materials for

Mechanism of spindle pole organization and instability in human oocytes

Chun So *et al.*

Corresponding author: Melina Schuh, melina.schuh@mpinat.mpg.de

Science **375**, eabj3944 (2022)
DOI: [10.1126/science.abj3944](https://doi.org/10.1126/science.abj3944)

The PDF file includes:

Figs. S1 to S14
Tables S1 and S2

Other Supplementary Material for this manuscript includes the following:

MDAR Reproducibility Checklist
Movies S1 to S18

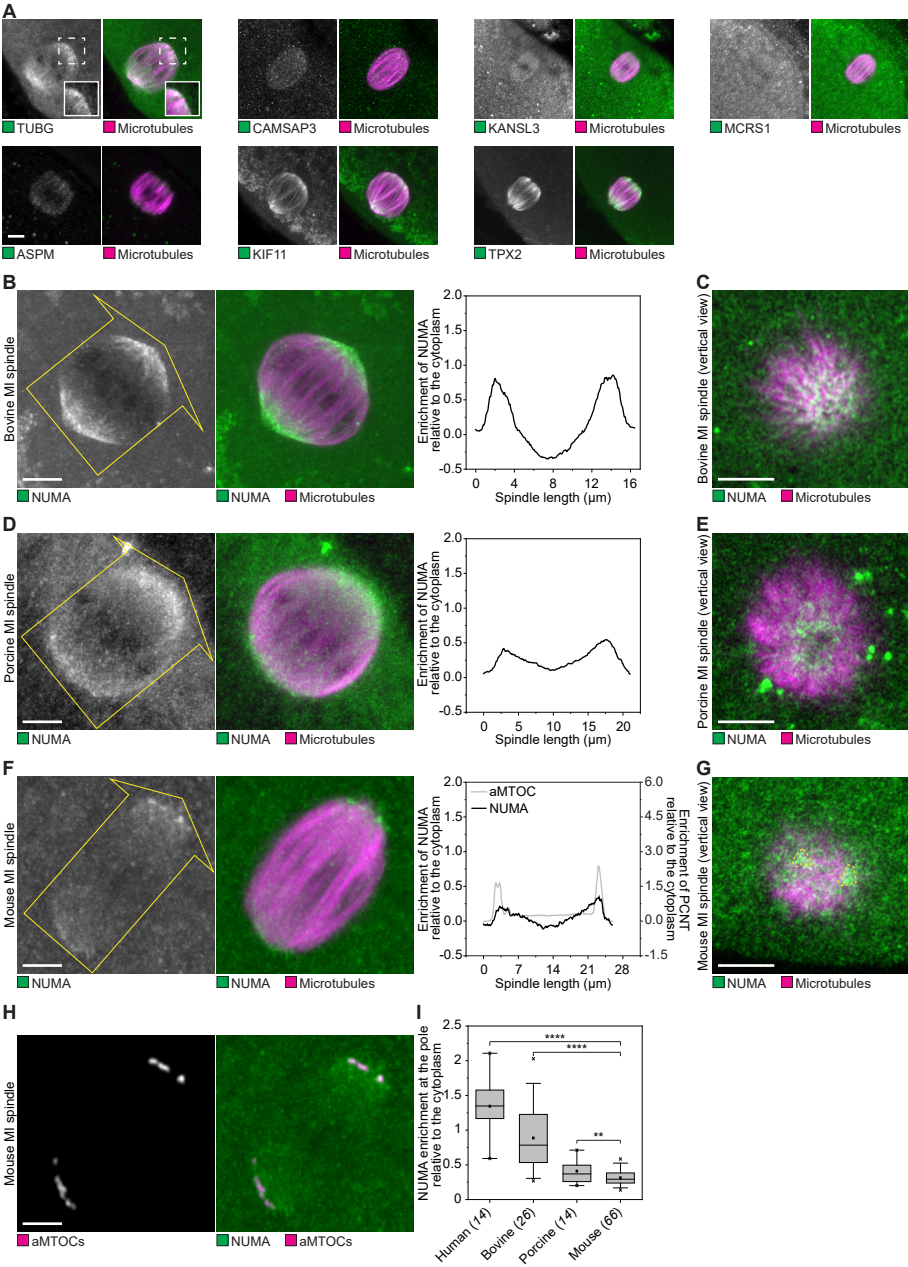


fig. S1

Fig. S1. NUMA is enriched at the spindle poles in mammalian oocytes, except in mouse oocytes. (A) Immunofluorescence images of human meiosis I (MI) and meiosis II (MII) spindles. Green, protein of interest; magenta, microtubules (α -tubulin). Insets are magnifications of a single z-section of regions marked by dashed line boxes. (B) Immunofluorescence images of a bovine MI spindle fixed at 12 hours after release. Green, NUMA; magenta, microtubules (α -tubulin). The graph is the fluorescence profile of NUMA across the spindle along the direction of the yellow arrow. (C) Immunofluorescence image of a bovine MI spindle fixed at 12 hours after release in a vertical orientation. Green, NUMA; magenta, microtubules (α -tubulin). (D) Immunofluorescence images of a porcine MI spindle fixed at 11 hours after release. Green, NUMA; magenta, microtubules (α -tubulin). The graph is the fluorescence profile of NUMA across the spindle along the direction of the yellow arrow. (E) Immunofluorescence image of a porcine MI spindle fixed at 11 hours after release in a vertical orientation. Green, NUMA; magenta, microtubules (α -tubulin). (F) Immunofluorescence images of a mouse MI spindle fixed at 7 hours after release. Green, NUMA; magenta, microtubules (α -tubulin). The graph is the fluorescence profile of NUMA and aMTOC (PCNT) across the spindle along the direction of the yellow arrow. (G) Immunofluorescence image of a mouse MI spindle fixed at 7 hours after release in a vertical orientation. Green, NUMA; magenta, microtubules (α -tubulin). aMTOCs are outlined with yellow dashed lines. (H) Immunofluorescence image of the same spindle in (F). Green, NUMA; magenta, aMTOCs (PCNT). (I) Quantification of NUMA enrichment at the spindle pole over the cytoplasm in different mammalian oocytes at MI. The number of poles analyzed is specified in italics. Scale bars, 5 μ m.

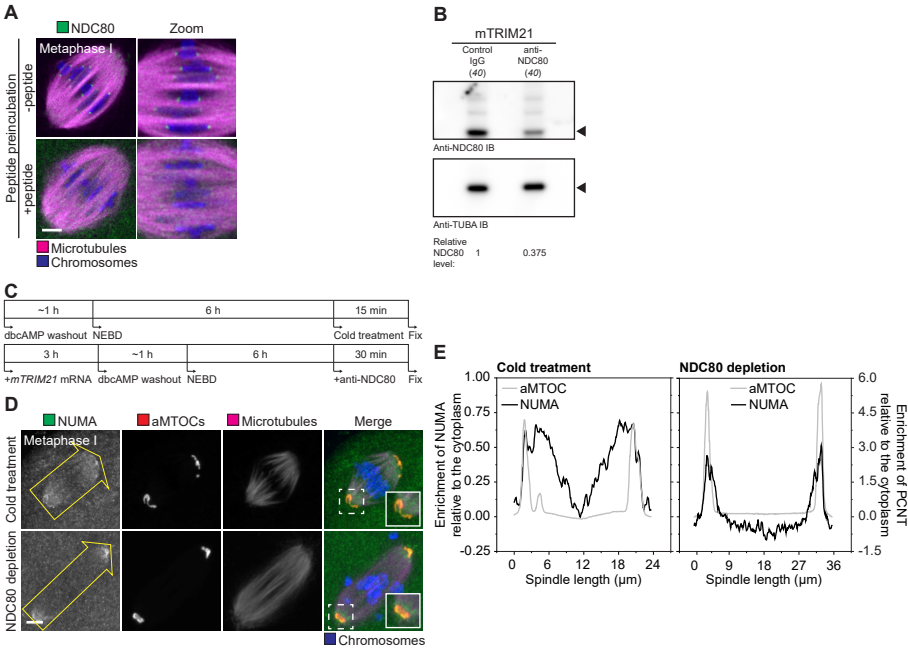


fig. S2

Fig. S2. Validation of the anti-NDC80/HEC1 antibody for Trim-Away and the localization of NUMA in cold-treated and NDC80-depleted mouse oocytes. (A) Immunofluorescence images of mouse MI spindles fixed at 7 hours after release, stained with non-preincubated and NDC80 peptide preincubated anti-NDC80. Green, NDC80; magenta, microtubules (α -tubulin); blue, chromosomes (Hoechst). (B) Immunoblots of control and NDC80-depleted mouse oocytes, lysed at 7 hours after release. Black arrows mark the band corresponding to each protein. The number of oocytes loaded is specified in italics. (C) Schematic diagrams of the experiments in (D). (D) Immunofluorescence images of MI spindles from cold-treated and acutely NDC80-depleted mouse oocytes, fixed at 7.25 or 7.5 hours after release. Green, NUMA; red, aMTOCs (PCNT); magenta, microtubules (α -tubulin); blue, chromosomes (Hoechst). Insets are magnifications of regions marked by dashed line boxes. (E) Fluorescence profile of NUMA and aMTOC (PCNT) across the spindles in (C) along the direction of the yellow arrows. Scale bars, 5 μ m.

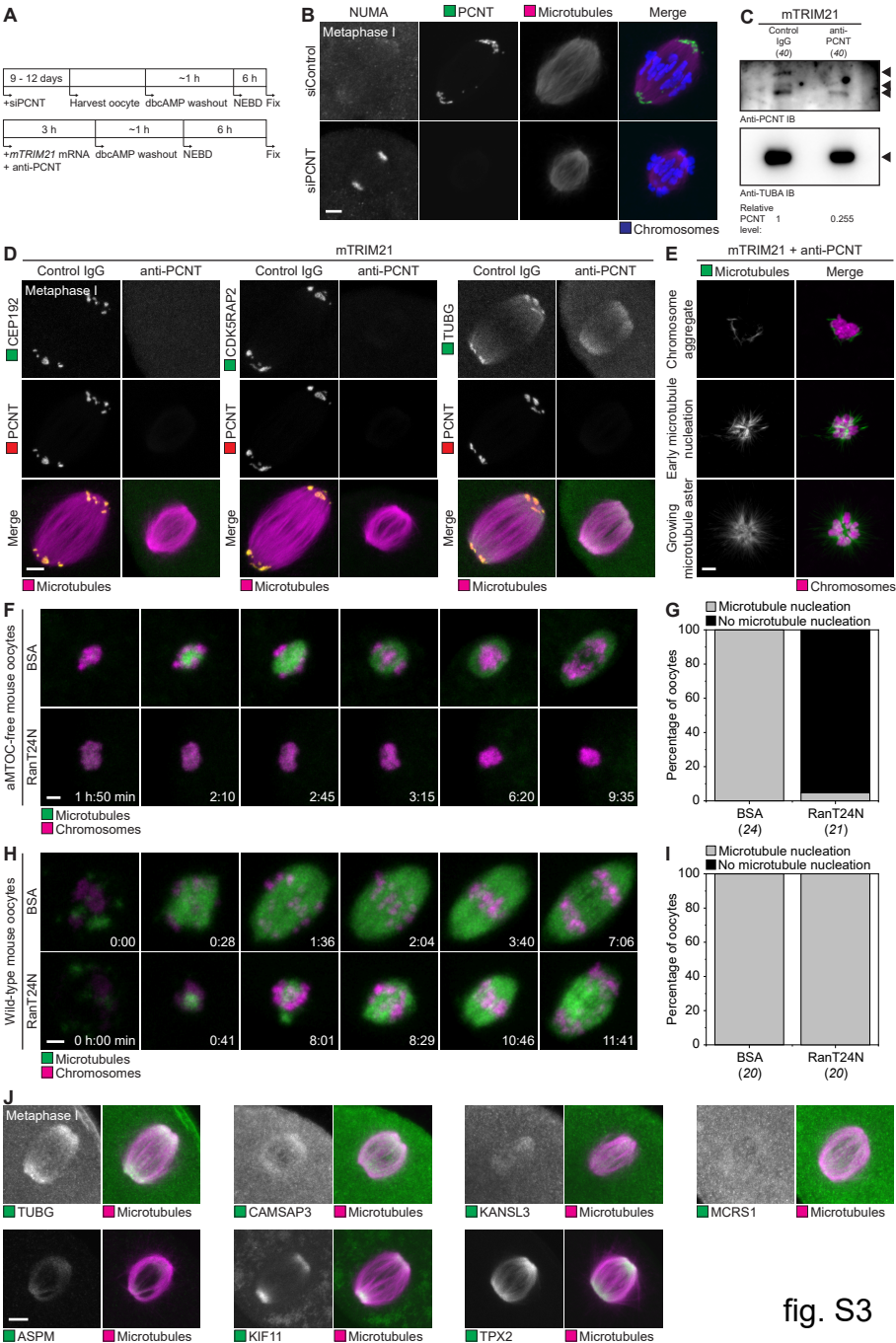


Fig. S3 Validation of the anti-PCNT antibody for Trim-Away and the characterization of aMTOC-free mouse oocytes. (A) Schematic diagrams of the experiments in (B) and (D). (B) Immunofluorescence images of MI spindles from control and PCNT-depleted mouse oocytes, fixed at 7 hours after release. Gray, NUMA; green, PCNT; magenta, microtubules (α -tubulin); blue, chromosomes (Hoechst). (C) Immunoblots of control and PCNT-depleted mouse oocytes, lysed at 7 hours after release. Black arrows mark the band corresponding to each protein. The number of oocytes loaded is specified in italics. The three arrows in anti-PCNT IB mark different isoforms of PCNT. (D) Immunofluorescence images of MI spindles from control and PCNT-depleted mouse oocytes, fixed at 7 hours after release. Green, protein of interest; red, PCNT; magenta, microtubules (α -tubulin). (E) Immunofluorescence images of aMTOC-free mouse oocytes fixed at different stages of meiosis I. Green, microtubules (α -tubulin); magenta, chromosomes (Hoechst). (F) Still images from time-lapse movies of aMTOC-free mouse oocytes treated with BSA and RanT24N. Green, microtubules (mClover3-MAP4-MTBD); magenta, chromosomes (H2B-miRFP). (G) Manual scoring (Fisher's exact test, ****) of microtubule nucleation in control and Ran-inhibited aMTOC-free mouse oocytes. (H) Still images from time-lapse movies of wild-type mouse oocytes treated with BSA and RanT24N. Green, microtubules (mClover3-MAP4-MTBD); magenta, chromosomes (H2B-miRFP). (I) Manual scoring (Fisher's exact test, N.S.) of microtubule nucleation in control and Ran-inhibited wild-type mouse oocytes. (J) Immunofluorescence images of MI spindles from aMTOC-free mouse oocytes, fixed at 7 hours after release. Green, protein of interest; magenta, microtubules (α -tubulin). Time is indicated as hours:minutes after nuclear envelope breakdown (NEBD). The number of oocytes analyzed is specified in italics. Scale bars, 5 μ m.

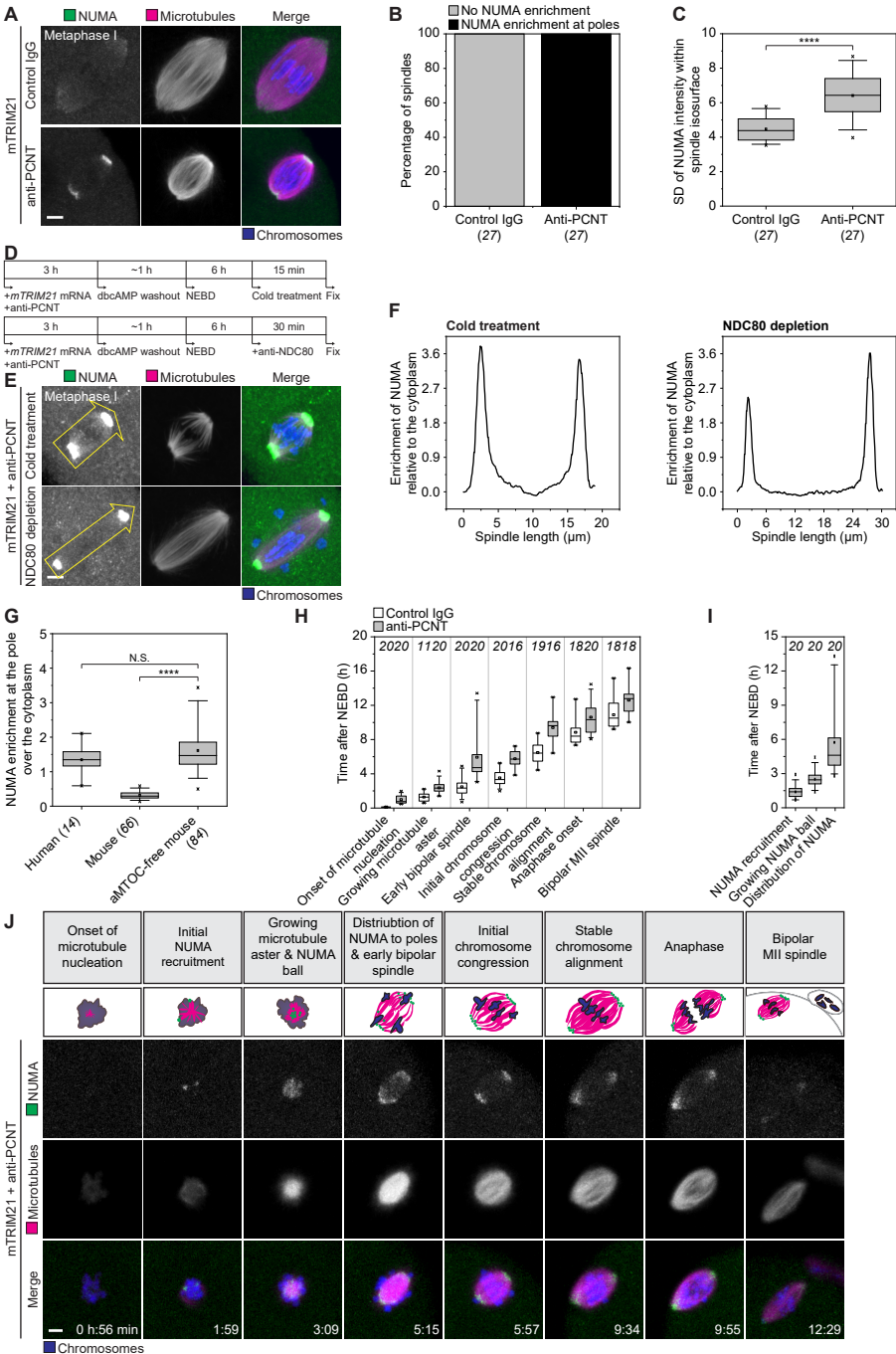


Fig. S4 Localization of NUMA in aMTOC-free mouse oocytes. (A) Immunofluorescence images of MI spindles from control and PCNT-depleted mouse oocytes, fixed at 7 hours after release. Green, NUMA; magenta, microtubules (α -tubulin); blue, chromosomes (Hoechst). (B and C) Manual scoring (Fisher's exact test, ****) and automated quantification of NUMA enrichment at poles in control and PCNT-depleted mouse MI oocytes. (D) Schematic diagrams of the experiments in (E). (E) Immunofluorescence images of MI spindles from cold-treated and acutely NDC80-depleted aMTOC-free mouse oocytes, fixed at 7.25 or 7.5 hours after release. Green, NUMA; magenta, microtubules (α -tubulin); blue, chromosomes (Hoechst). (F) Fluorescence profile of NUMA across the spindles in (E) along the direction of the yellow arrows. (G) Quantification of NUMA enrichment at the spindle pole over the cytoplasm in human, wild-type and aMTOC-free mouse oocytes at MI. (H and I) Quantification of the time of different stages of meiosis in control and PCNT-depleted mouse oocytes. (J) Still images from a time-lapse movie of an aMTOC-free mouse oocyte. Green, mClover3-NUMA; magenta, microtubules (mClover3-MAP4-MTBD); blue, chromosomes (H2B-miRFP). Time is indicated as hours:minutes after NEBD. The number of oocytes or poles analyzed is specified in italics. Scale bars, 5 μ m.

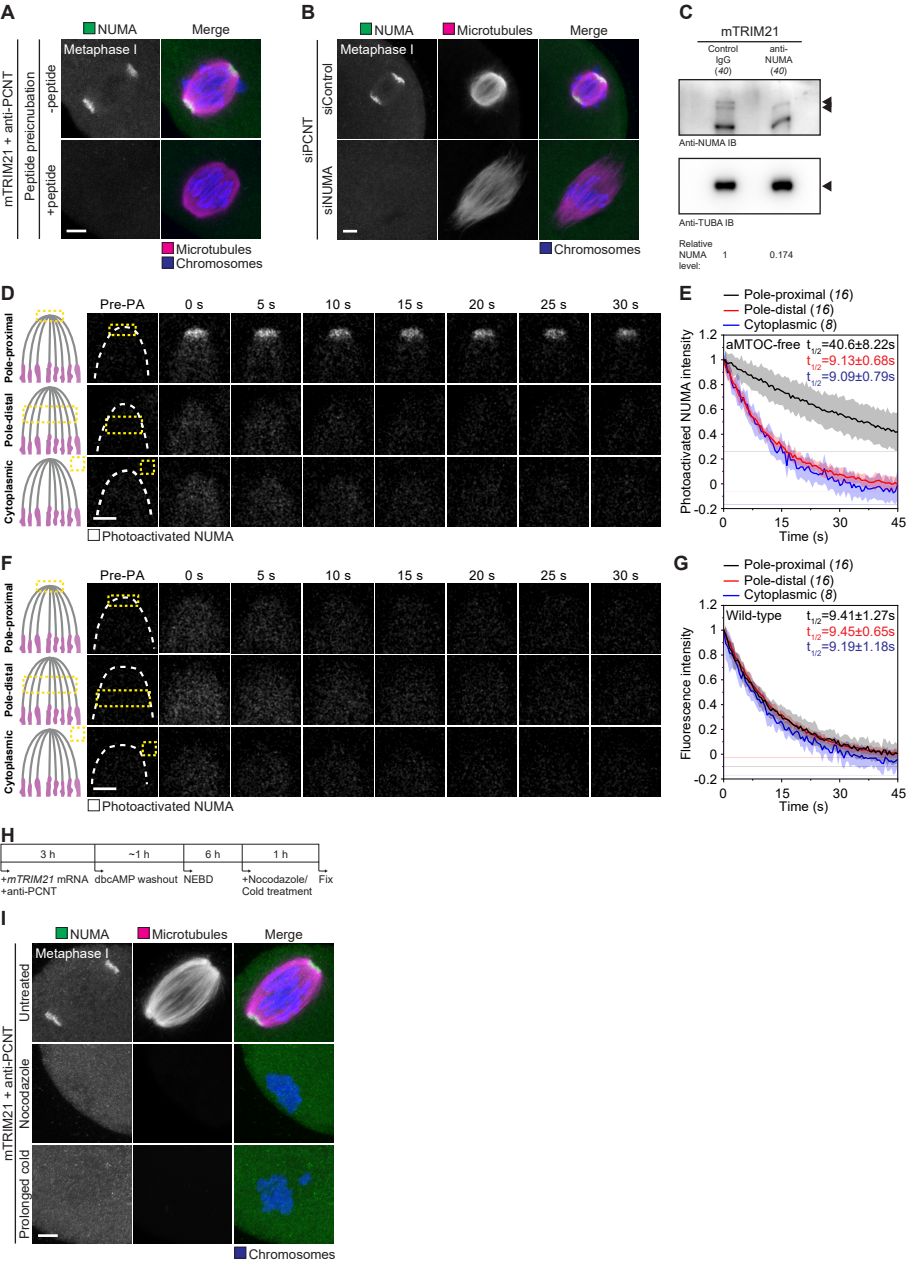


fig. S5

Fig. S5 Validation of the anti-NUMA antibody for Trim-Away and the photoactivation of NUMA in wildtype and aMTOC-free mouse oocytes. (A) Immunofluorescence images of MI spindles from aMTOC-free mouse oocytes fixed at 7 hours after release, stained with non-preincubated and NUMA peptide preincubated anti-NUMA. Green, NUMA; magenta, microtubules (α -tubulin); blue, chromosomes (Hoechst). (B) Immunofluorescence images of MI spindles from control and NUMA-depleted aMTOC-free mouse oocytes, fixed at 7 hours after release. Green, NUMA; magenta, microtubules (α -tubulin); blue, chromosomes (Hoechst). (C) Immunoblots of control and NUMA-depleted mouse oocytes, lysed at 7 hours after release. Black arrows mark the band corresponding to each protein. The number of oocytes loaded is specified in italics. The two arrows in anti-NUMA IB mark NUMA with and without post-translational modifications. (D) Photoactivation (PA) of NUMA in different regions of MI spindles from aMTOC-free mouse oocytes at 6 hours after NEBD. (E) Dissipation and half-life of photoactivated NUMA at different regions of MI spindles from aMTOC-free mouse oocytes. (F) PA of NUMA in different regions of MI spindles from wildtype mouse oocytes at 6 hours after NEBD. (G) Dissipation and half-life of photoactivated NUMA at different regions of MI spindles from wildtype mouse oocytes. (H) Schematic diagram of the experiment in (I). (I) Immunofluorescence images of untreated, nocodazole-treated and prolonged cold-treated aMTOC-free mouse MI oocytes, fixed at 8 hours after release. Green, NUMA; magenta, microtubules (α -tubulin); blue, chromosomes (Hoechst). Spindle poles are outlined with white dashed lines; photoactivated areas are outlined by yellow dashed line boxes. Time is indicated as seconds after photoactivation. Error bars (shaded areas) represent SD. The number of poles analyzed is specified in italics. Scale bars, 5 μ m.

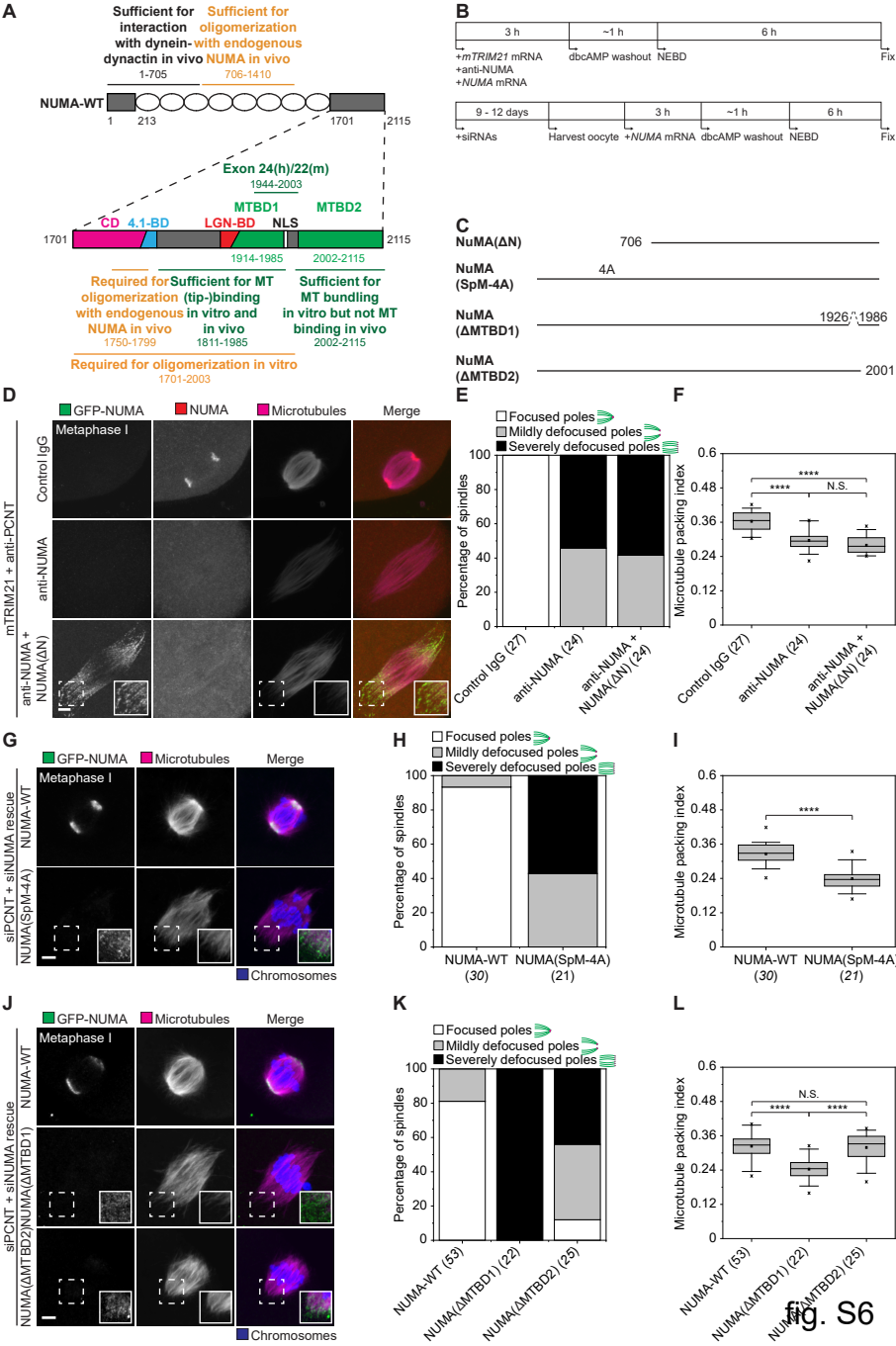


Fig. S6 Requirement of different domains of NUMA for pole focusing in aMTOC-free mouse oocytes. (A) Schematic diagram of different domains in NUMA. ‘CD’ indicates the (membrane) clustering domain; ‘4.1-BD’ indicates the protein 4.1-binding domain; ‘LGN-BD’ indicates the LGN-binding domain; ‘MTBD’ indicates the microtubule binding domain. ‘NLS’ indicates the nuclear localization signal. (B) Schematic diagram of the experiments in (D), (G) and (J). (C) Schematic diagram of NUMA mutants used in this study. (D) Immunofluorescence images of MI spindles from control, NUMA-depleted and NUMA(Δ N)-NUMA-depleted aMTOC-free mouse oocytes, fixed at 7 hours after release. Green, GFP-NUMA; red, NUMA; magenta, microtubules (α -tubulin). (E and F) Manual scoring (Fisher’s exact test, **** for control versus NUMA(Δ N)-NUMA-depleted) and automated quantification of spindle pole defocusing in control, NUMA-depleted and NUMA(Δ N)-NUMA-depleted aMTOC-free mouse oocytes. (G) Immunofluorescence images of MI spindles from NUMA-depleted aMTOC-free mouse oocytes rescued with NUMA-WT and NUMA(SpM-4A), fixed at 7 hours after release. Green, GFP-NUMA; magenta, microtubules (α -tubulin); blue, chromosomes (Hoechst). (H and I) Manual scoring (Fisher’s exact test, ****) and automated quantification of spindle pole defocusing in aMTOC-free mouse MI oocytes rescued with NUMA-WT and NUMA(SpM-4A). (J) Immunofluorescence images of MI spindles from NUMA-depleted aMTOC-free mouse oocytes rescued with NUMA-WT, NUMA(Δ MTBD1) and NUMA(Δ MTBD2), fixed at 7 hours after release. Green, GFP-NUMA; magenta, microtubules (α -tubulin); blue, chromosomes (Hoechst). (K and L) Manual scoring (Fisher’s exact test, **** for NUMA-WT versus both NUMA(Δ MTBD1) and NUMA(Δ MTBD2)) and automated quantification of spindle pole defocusing in aMTOC-free mouse MI oocytes rescued with NUMA-WT, NUMA(Δ MTBD1) and

NUMA(Δ MTBD2). Insets are magnifications of regions marked by dashed line boxes. The number of oocytes analyzed is specified in italics. Scale bars, 5 μ m.

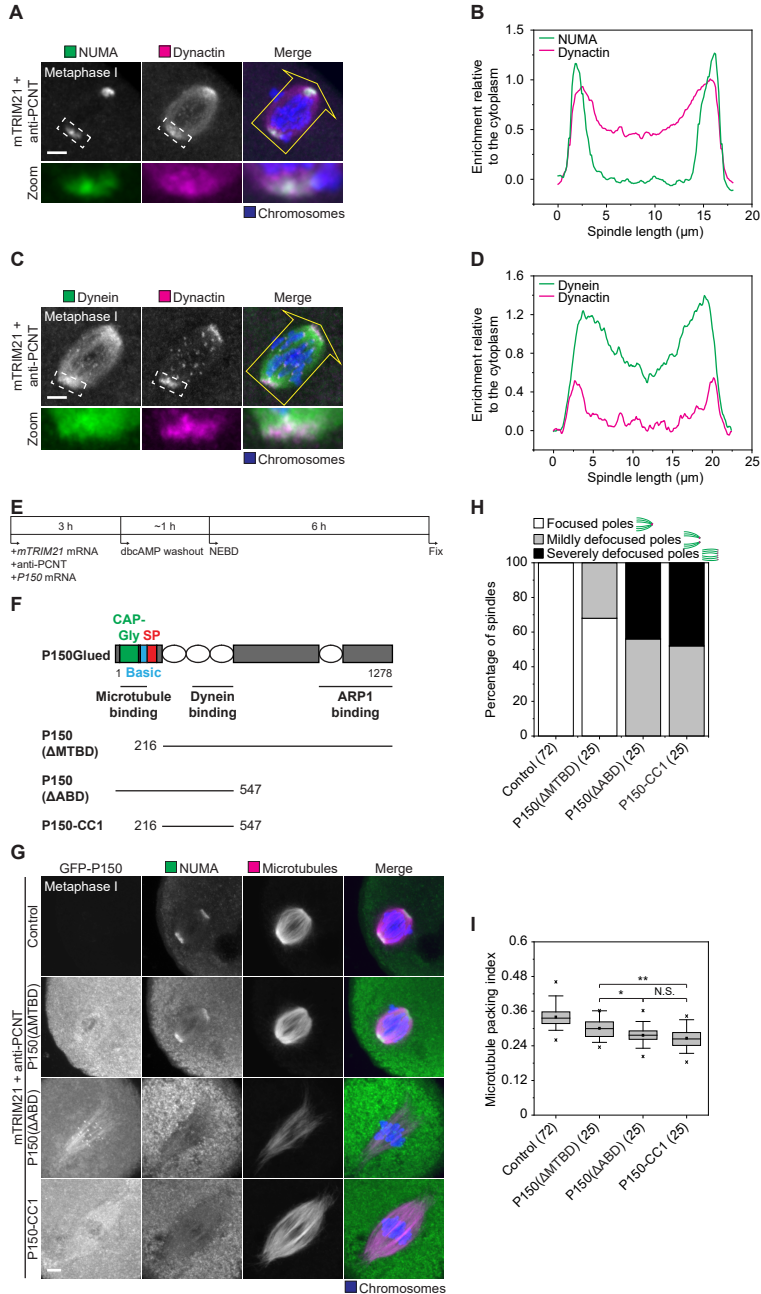


fig. S7

Fig. S7 Localization of dynein and dynactin in aMTOC-free mouse oocytes and validation of P150-CC1-mediated inhibition. (A) Immunofluorescence images of the MI spindle from an aMTOC-free mouse oocytes fixed at 7 hours after release. Green, NUMA; magenta, dynactin (P150); blue, chromosomes (Hoechst). (B) Fluorescence profile of NUMA and dynactin across the spindle in (A) along the direction of the yellow arrow. (C) Immunofluorescence images of the MI spindle from an aMTOC-free mouse oocytes fixed at 7 hours after release. Green, dynein (DHC); magenta, dynactin (P150); blue, chromosomes (Hoechst). (D) Fluorescence profile of dynein and dynactin across the spindle in (C) along the direction of the yellow arrow. (E) Schematic diagram of the experiment in (G). (F) Schematic diagram of different domains in P150 and P150 mutants used in this study. ‘CAP-Gly’ indicates the cytoskeleton-associated protein/glycine-rich domain; ‘Basic’ indicates the basic domain; ‘SP’ indicates the serine/proline-rich domain. (G) Immunofluorescence images of MI spindles from aMTOC-free mouse oocytes overexpressing P150(Δ MTBD), P150(Δ ABD) and P150-CC1, fixed at 7 hours after release. Gray, GFP-P150; green, NUMA; magenta, microtubules (α -tubulin); blue, chromosomes (Hoechst). (H and I) Manual scoring (Fisher’s exact test, **** for P150(Δ MTBD) versus both P150(Δ ABD) and P150-CC1) and automated quantification of spindle pole defocusing in aMTOC-free mouse MI oocytes overexpressing P150(Δ MTBD), P150(Δ ABD) and P150-CC1. The number of oocytes analyzed is specified in italics. Scale bars, 5 μ m.

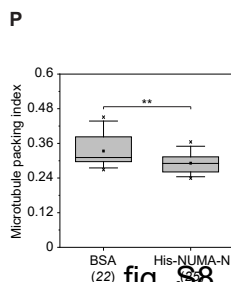
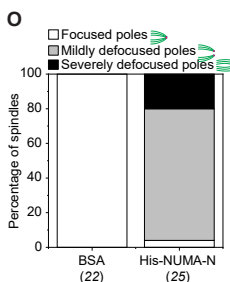
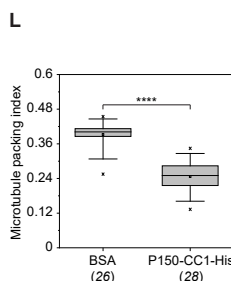
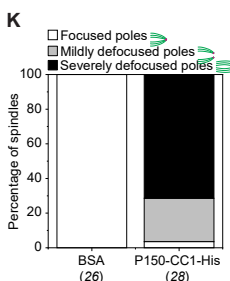
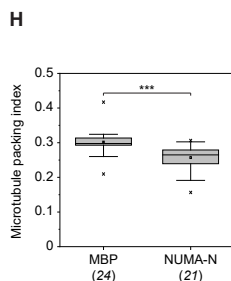
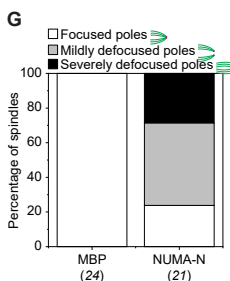
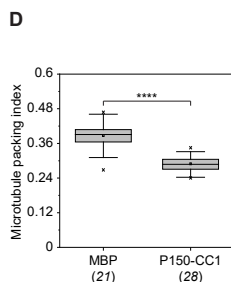
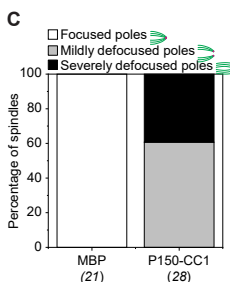
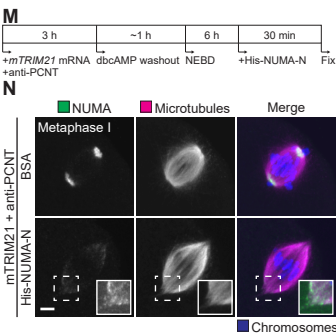
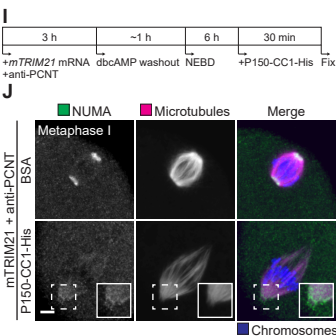
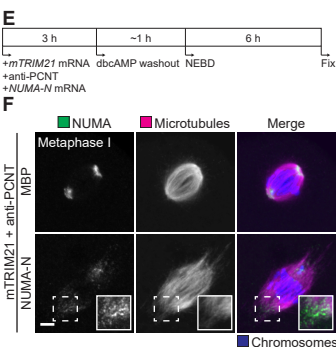
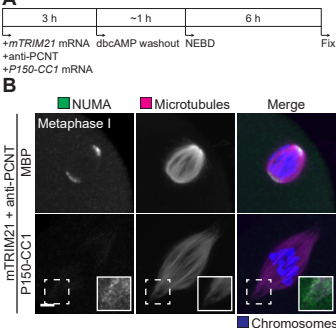


Fig. S8 Requirement of dynein-dynactin for pole focusing in aMTOC-free mouse oocytes.

(A) Schematic diagram of the experiment in (B). (B) Immunofluorescence images of MI spindles from aMTOC-free mouse oocytes treated with MBP and P150-CC1 from NEBD, fixed at 7 hours after release. (C and D) Manual scoring (Fisher's exact test, ****) and automated quantification of spindle pole defocusing in control and P150-CC1-treated aMTOC-free mouse MI oocytes. (E) Schematic diagram of the experiment in (F). (F) Immunofluorescence images of MI spindles from aMTOC-free mouse oocytes treated with MBP and NUMA-N from NEBD, fixed at 7 hours after release. (G and H) Manual scoring (Fisher's exact test, ****) and automated quantification of spindle pole defocusing in control and NUMA-N-treated aMTOC-free mouse MI oocytes. (I) Schematic diagram of the experiment in (J). (J) Immunofluorescence images of MI spindles from aMTOC-free mouse oocytes acutely treated with BSA and P150-CC1-His, fixed at 7.5 hours after release. (K and L) Manual scoring (Fisher's exact test, ****) and automated quantification of spindle pole defocusing in control and acutely P150-CC1-His-treated aMTOC-free mouse MI oocytes. (M) Schematic diagram of the experiment in (N). (N) Immunofluorescence images of MI spindles from aMTOC-free mouse oocytes acutely treated with BSA and His-NUMA-N, fixed at 7.5 hours after release. (O and P) Manual scoring (Fisher's exact test, ****) and automated quantification of spindle pole defocusing in control and acutely His-NUMA-N treated aMTOC-free mouse MI oocytes. Insets are magnifications of regions marked by dashed line boxes. The number of oocytes analyzed is specified in italics. Scale bars, 5 μ m.

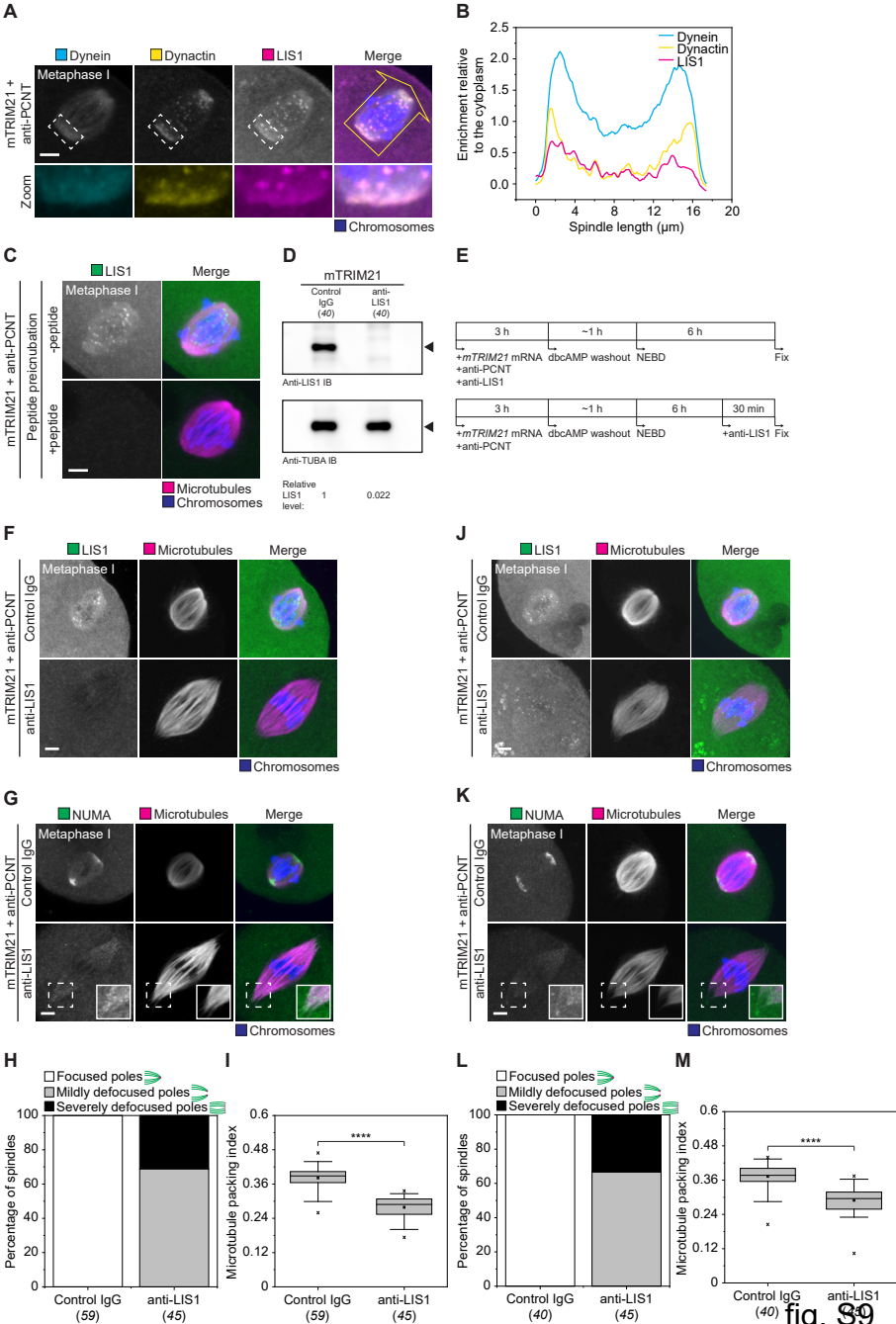
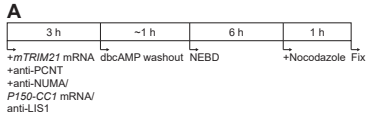


Fig. S9 Validation of the anti-LIS1 antibody for Trim-Away and the requirement of LIS1 for pole focusing in aMTOC-free mouse oocytes. (A) Immunofluorescence images of the MI spindle from an aMTOC-free mouse oocytes, fixed at 7 hours after release. Cyan, dynein (DHC); yellow, dynactin (P150); magenta, LIS1; blue, chromosomes (Hoechst). (B) Fluorescence profile of dynein, dynactin and LIS1 across the spindle in (A) along the direction of the yellow arrow. (C) Immunofluorescence images of MI spindles from aMTOC-free mouse oocytes fixed at 7 hours after release, stained with non-preincubated and LIS1 peptide preincubated anti-LIS1. Green, LIS1; magenta, microtubules (α -tubulin); blue, chromosomes (Hoechst). (D) Immunoblots of control and LIS1-depleted mouse oocytes lysed at 7 hours after release. Black arrows mark the band corresponding to each protein. The number of oocytes loaded is specified in italics. (E) Schematic diagrams of the experiments in (F), (G), (J) and (K). (F and G) Immunofluorescence images of MI spindles from control and LIS1-depleted aMTOC-free mouse oocytes, fixed at 7 hours after release. Green, LIS1 or NUMA; magenta, microtubules (α -tubulin); blue, chromosomes (Hoechst). (H and I) Manual scoring (Fisher's exact test, ****) and automated quantification of spindle pole defocusing in control and LIS1-depleted aMTOC-free mouse MI oocytes. (J and K) Immunofluorescence images of MI spindles from control and acutely LIS1-depleted aMTOC-free mouse oocytes, fixed at 7.5 hours after release. Green, LIS1 or NUMA; magenta, microtubules (α -tubulin); blue, chromosomes (Hoechst). (L and M) Manual scoring (Fisher's exact test, ****) and automated quantification of spindle pole defocusing in control and acutely LIS1-depleted aMTOC-free mouse MI oocytes. Insets are magnifications of regions marked by dashed line boxes. The number of oocytes analyzed is specified in italics. Scale bars, 5 μ m.



B

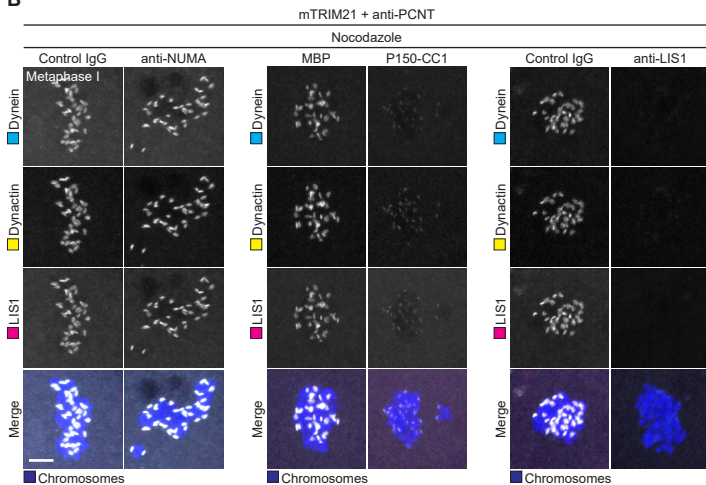


Fig. S10 Dynein, dynactin and LIS1 function together. (A) Schematic diagram of the experiments in (B). (B) Immunofluorescence images of control, NUMA-depleted, P150-CC1-treated and LIS1-depleted aMTOC-free mouse MI oocytes treated with nocodazole, fixed at 8 hours after release. Cyan, dynein (DHC); yellow, dynactin (P150); magenta, LIS1; blue, chromosomes (Hoechst). Scale bars, 5 μ m.

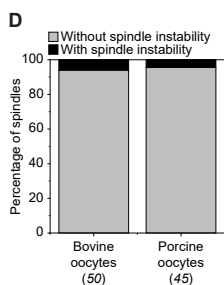
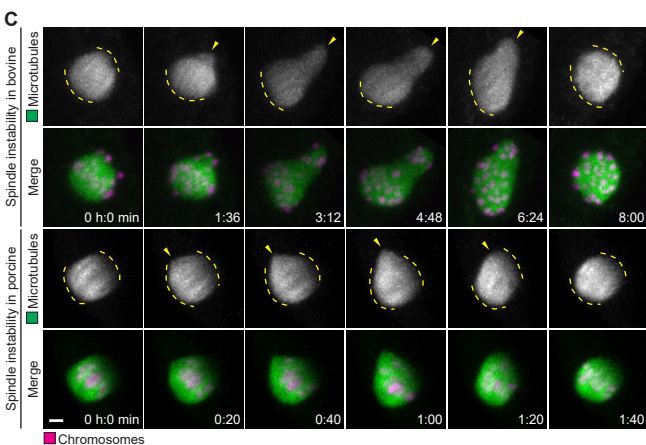
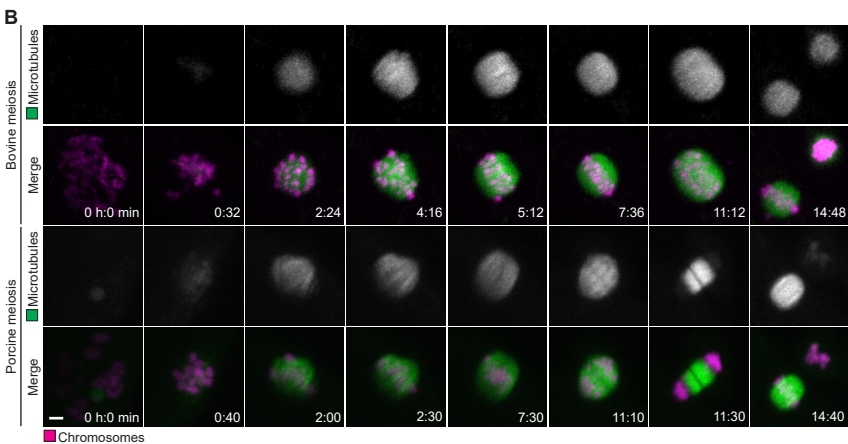
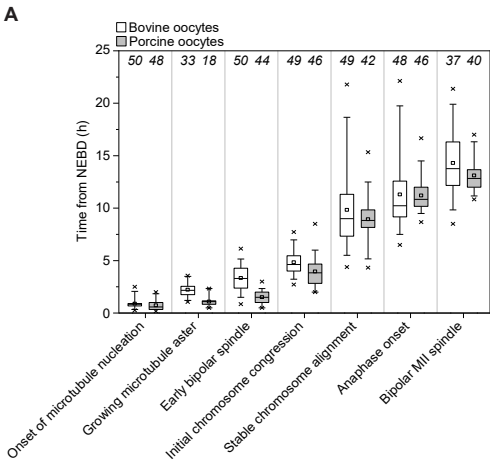


fig. S11

Fig. S11. Spindle instability is not a feature of meiosis I in bovine and porcine oocytes. (A) Quantification of the time of different stages of meiosis in bovine and porcine oocytes. **(B)** Still images from time-lapse movies of bovine and porcine oocytes assembling a stable spindle. Green, microtubules (EGFP-MAP4); magenta, chromosomes (H2B-mCherry). Time is indicated as hours:minutes after NEBD. **(C)** Still images from time-lapse movies of bovine and porcine oocytes assembling an unstable spindle. Green, microtubules (EGFP-MAP4); magenta, chromosomes (H2B-mCherry). Time is indicated as hours: minutes after the onset of spindle instability. Dashed lines highlight stable spindle poles. Arrowheads highlight unstable spindle poles. **(D)** Manual scoring of spindle instability in bovine and porcine oocytes. The number of oocytes analyzed is specified in italics. Scale bars, 5 μ m.

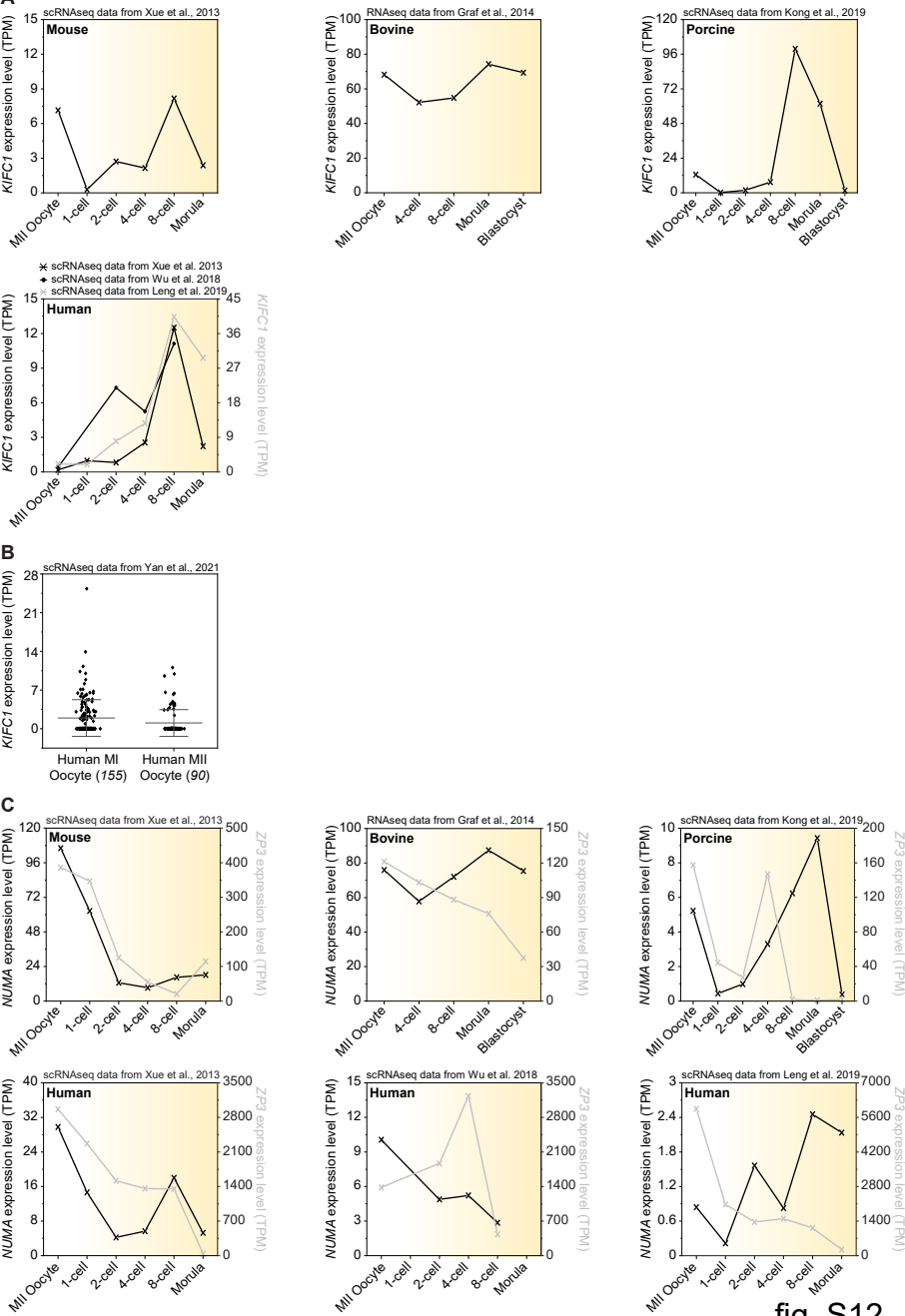


fig. S12

Fig. S12 *KIFC1/HSET* mRNA is barely detectable in human oocytes, but not in oocytes of other mammalian species. (A) *KIFC1* mRNA levels in MII oocytes and preimplantation embryos from mice, cows, pigs and humans. (B) *KIFC1* mRNA levels in MI and MII oocytes from humans. The number of oocytes analyzed is specified in italics. (C) *NUMA* and *ZP3* mRNA levels in MII oocytes and preimplantation embryos from mice, cows, pigs and humans.

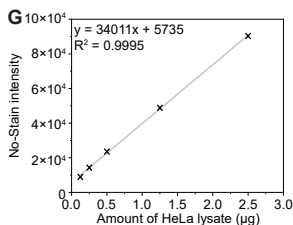
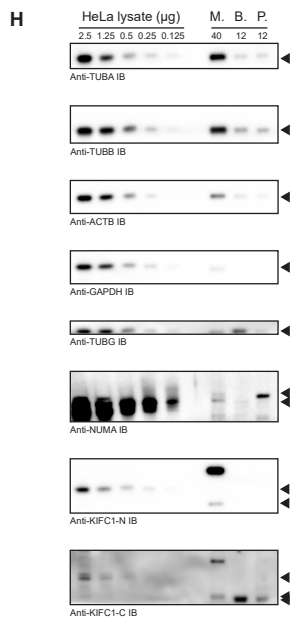
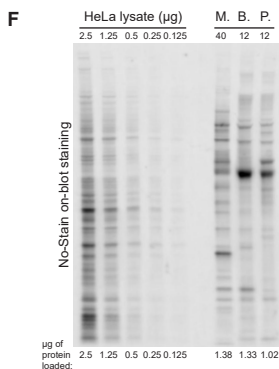
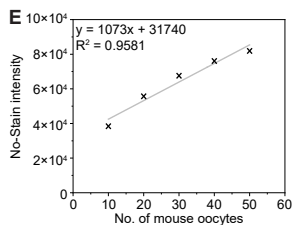
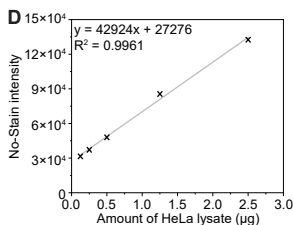
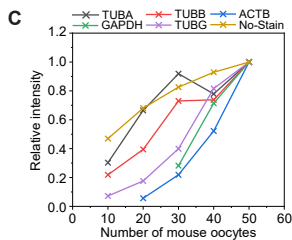
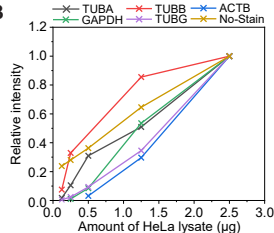
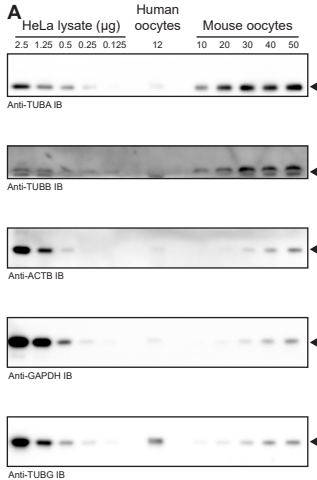


Fig. S13 Validation of on-blot total protein normalization and the detection of KIFC1 protein in mouse, bovine and porcine oocytes. (A) Immunoblots of HeLa cell, human oocyte and mouse oocyte lysates for canonical housekeeping proteins. The amount of HeLa cell lysate or the number of oocytes loaded is indicated above each lane. (B and C) Quantification of the intensity of canonical housekeeping proteins in different amount of HeLa cell lysate and different number of mouse oocytes. (D and E) Calibration curves for on-blot No-Stain protein staining in Fig. 4B for different amount of HeLa cell lysate and different number of mouse oocytes. (F) No-Stain protein staining for the blot of HeLa cell, mouse oocyte, bovine oocyte and porcine oocyte lysates. ‘M.’ indicates mouse oocytes; ‘B.’ indicates bovine oocytes; ‘P.’ indicates porcine oocytes. The amount of HeLa cell lysate or the number of oocytes loaded is indicated above each lane. The corresponding amount of protein loaded is indicated under each lane. (G) Calibration curve for on-blot No-Stain protein staining in (F). (H) Immunoblots of HeLa cell, mouse oocyte, bovine oocyte and porcine oocyte lysates. Mouse, bovine and porcine oocytes were lysed at 7, 12 and 11 hours after release, respectively. Note that the anti-KIFC1-N antibody recognized human and mouse KIFC1, but not bovine and porcine KIFC1. Black arrows mark the band corresponding to each protein.

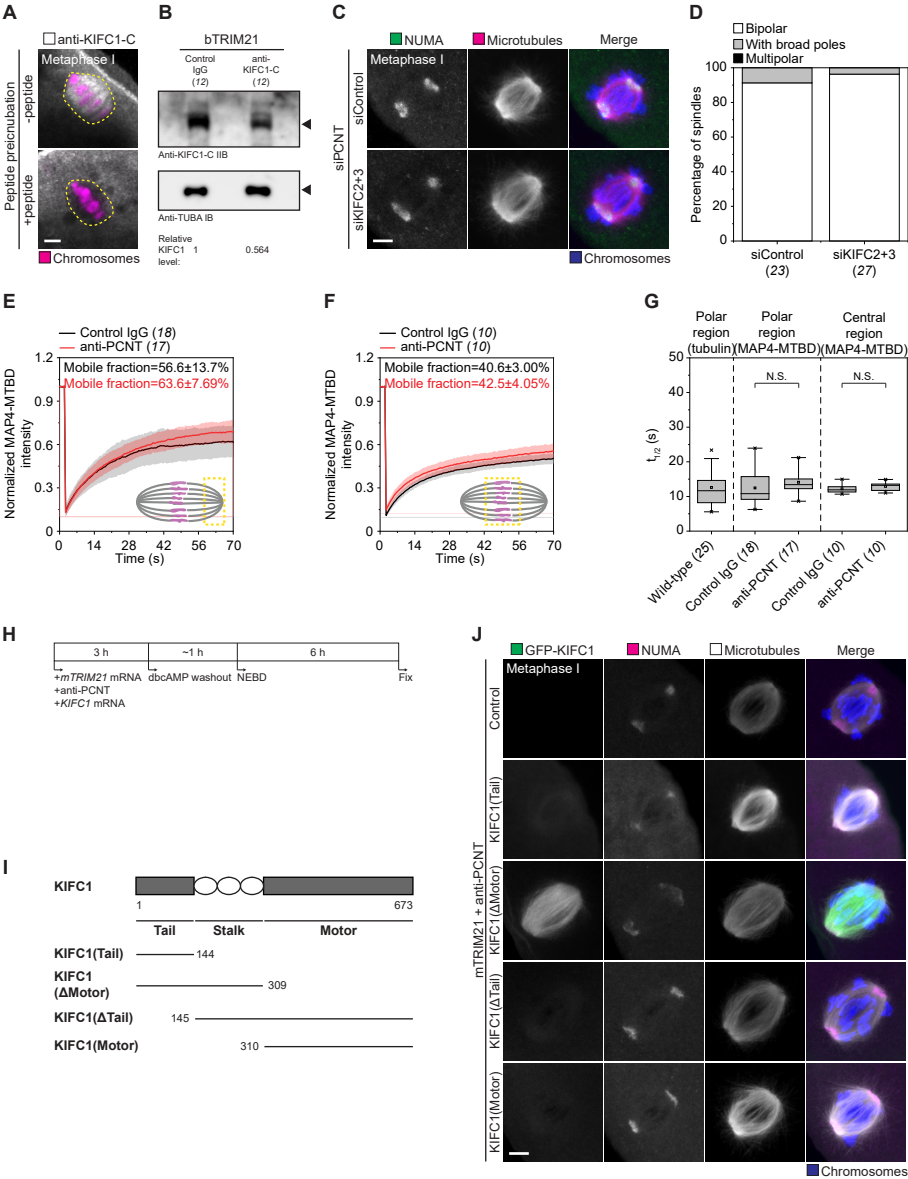


fig. S14

Fig. S14 Validation of the anti-KIFC1 antibody for Trim-Away and the characterization of KIFC1 in aMTOC-free mouse oocytes. (A) Immunofluorescence images of MI spindles from bovine oocytes fixed at 12 hours after release, stained with non-preincubated and KIFC1 peptide preincubated anti-KIFC1-C. Gray, KIFC1; magenta, chromosomes (Hoechst). (B) Immunoblots of control and KIFC1-depleted bovine oocytes lysed at 12 hours after release. Black arrows mark the band corresponding to each protein. The number of oocytes loaded is specified in italics. (C) Immunofluorescence images of MI spindles from control and KIFC2+3-depleted aMTOC-free mouse oocytes, fixed at 7 hours after release. Green, NUMA; magenta, microtubules (α -tubulin); blue, chromosomes (Hoechst). (D) Manual scoring of spindle polarity in control and KIFC2+3-depleted aMTOC-free mouse MI oocytes (Fisher's exact test, N.S.). (E) Recovery of photobleached mScarlet-MAP4-MTBD at the spindle poles in control and PCNT-depleted mouse MI oocytes at 6 hours after NEBD. (F) Recovery of photobleached mScarlet-MAP4-MTBD in the central region of the spindle in control and PCNT-depleted mouse MI oocytes at 6 hours after NEBD. Error bars (shaded areas) represent SD. (G) Half-life of α -tubulin and mScarlet-MAP4-MTBD at different regions of MI spindles from control and PCNT-depleted mouse oocytes. (H) Schematic diagram of the experiment in (J). (I) Schematic diagram of different domains in KIFC1 and KIFC1 mutants used in this study. (J) Immunofluorescence images of MI spindles from aMTOC-free mouse oocytes overexpressing KIFC1(Tail), KIFC1(Δ Motor), KIFC1(Δ Tail) and KIFC1(Motor), fixed at 7 hours after release. Green, GFP-KIFC1; magenta, NUMA; gray, microtubules (α -tubulin); blue, chromosomes (Hoechst). The number of oocytes or poles analyzed is specified in italics. Scale bars, 5 μ m.

Table S1. Details of donors of all human oocytes used in this study.

Donor number	Age	BMI	Cause of infertility	No. of GV oocyte(s)	No. of MI oocyte(s)	Used in
1	43	25.9	Unknown	0	1	Immunofluorescence
2	28	30.1	Unknown	4	0	
3	30	24.8	Unknown	6	0	
4	36	23.3	Unknown	1	0	
5	27	21.1	Male	0	1	
6	31	24.5	Male	0	2	
7	30	32.6	Other	5	2	
8	28	18.8	Male	4	0	
9	36	27.0	Male	1	0	
10	38	22.7	Other	1	0	
11	37	27.1	Male	3	0	
12	35	29.4	Male	0	1	
13	34	29.3	Male	1	1	
14	39	21.5	Male	7	0	
15	39	31.8	Male	2	0	
16	35	22.2	Male	1	0	Experimental group for P150-CC1 inhibition
17	41	24.4	Male	2	0	Immunofluorescence
18	34	30.4	Male	7	0	Control and experimental groups for P150-CC1 inhibition
19	35	26.0	Unknown	2	0	Immunofluorescence
20	35	24.8	Male	1	1	
21	35	32.4	Unknown	3	0	Control and experimental groups for P150-CC1 inhibition
22	44	24.9	Unknown	1	0	Experimental group for P150-CC1 inhibition
23	33	26.4	Male	0	2	Immunofluorescence
24	39	29.6	Other	1	1	
25	30	27.7	Male	2	2	
26	33	30.3	Unknown	0	1	
27	40	24.7	Unknown	2	0	
28	37	21.6	Unknown	2	3	Control and experimental groups for P150-CC1 inhibition (GVs); Immunofluorescence (MIs)
29	40	?	Unknown	3	0	Control and experimental groups for P150-CC1 inhibition
30	27	21.4	Female	0	1	

31	41	24.1	Other	0	1	Immunofluorescence
32	39	21.0	Unknown	0	1	
33	32	26.5	Female	0	2	
34	28	25.0	Other	1	0	Control group for P150-CC1 inhibition
35	39	30.3	Male	1	0	Experimental group for P150-CC1 inhibition
36	31	28.0	Male + Female	1	0	Experimental group for P150-CC1 inhibition
37	33	33.1	Male	1	0	Immunofluorescence
38	34	24.5	Other	3	0	
39	37	26.7	Unknown	1	0	Experimental group for P150-CC1 inhibition
40	39	24.1	Unknown	2	0	Immunofluorescence
41	34	20.6	Male	2	0	Control group for P150-CC1 inhibition
42	30	29.1	Unknown	1	0	Experimental group for P150-CC1 inhibition
43	33	23.8	Unknown	1	0	Immunofluorescence
44	41	27.7	Male	1	0	
45	28	30.1	Male	1	0	
46	34	26.9	Unknown	1	0	
47	40	19.5	Male	2	0	
48	35	30.9	Female	3	1	
49	26	28.4	Male	1	0	
50	37	27.0	Unknown	0	3	
51	29	25.6	Unknown	4	0	
52	40	27.6	Unknown	2	0	
53	33	22.2	Male	3	0	
54	41	20.3	Male	0	4	
55	29	30.1	Male	1	0	
56	39	19.4	Female	0	1	
57	38	30.1	Male	0	1	
58	27	25.5	Male	1	0	
59	30	23.4	Male	1	0	Control group for NUMA Trim-Away
60	40	23.4	Unknown	1	0	Experimental group for NUMA Trim-Away
61	34	26.0	Male	2	0	Control group for NUMA Trim-Away
62	39	30.1	Male	2	0	Immunofluorescence
63	36	21.0	Male	2	0	
64	29	22.5	Male	1	0	Experimental group for NUMA Trim-Away
65	39	27.9	Unknown	3	0	Immunofluorescence

66	39	24.5	Other	1	0	Experimental group for NUMA Trim-Away
67	37	28.6	Male	3	0	Control group for NUMA Trim-Away
68	30	23.7	Unknown	1	0	Immunofluorescence
69	27	24.9	Male + Female	0	1	
70	35	22.8	Male	2	0	Control and experimental groups for NUMA Trim-Away
71	37	24.7	Unknown	2	0	Experimental group for NUMA Trim-Away
72	35	23.2	Unknown	0	1	Immunofluorescence
73	26	21.2	Other	0	1	
74	36	31.1	Unknown	0	2	
75	36	23.9	Unknown	2	1	
76	36	20.6	Unknown	2	0	
77	32	25.1	Male	3	0	
78	32	33.8	Other	1	1	
79	31	26.1	Male	7	0	Control and experimental groups for KIFC1 introduction
80	38	21.0	Male	3	0	Immunofluorescence
81	35	25.0	Female	1	0	
82	30	25.5	Male	1	0	
83	32	20.8	Male	2	0	
84	36	26.8	Male	1	0	
85	31	20.2	Male	1	0	
86	31	22.5	Other	1	0	
87	36	21.9	Male + Female	1	0	Immunofluorescence
88	33	25.8	Male	5	0	
89	34	24.8	Male	1	0	
90	32	25.2	Male	4	0	
91	30	25.3	Male	1	0	
92	34	23.1	Male	1	0	
93	30	23.4	Male	2	0	
94	35	17.7	Male	3	0	
95	34	20.0	Male	2	0	
96	33	24.4	Male	1	0	
97	38	?	Male	13	0	
98	34	?	Unknown	4	0	Control and experimental groups for KIFC1 introduction
99	38	?	Unknown	5	0	Immunofluorescence
100	39	?	Unknown	5	0	
101	33	?	Unknown	5	0	Control and experimental groups for KIFC1 introduction

102	35	?	Unknown	4	0	Control and experimental groups for KIFC1 introduction
103	35	?	Unknown	4	0	Control and experimental groups for KIFC1 introduction
Average age: 34.4 ± 4.1						
Average BMI: 25.3 ± 3.6						
Cause of infertility: 49.5% Male factor, 4.9% Female factor, 2.9% Male + Female factor, 9.7% Other factors and 33.0% Unknown						

Table S2. siRNAs used in this study.

Target gene	Name	Sequence
ASPM	Mm_Calmbp1_1	AAGGTTGAAATCGAAATTGAA
	Mm_Calmbp1_2	TTGGAATTTCTTATTAGTAAA
	Mm_Calmbp1_3	CAGGAGGGTTCTAGCATCTTA
	Mm_Calmbp1_4	CACAAGAAATATCTAACTTTA
CENPE	Mm_Cenpe_2	CAAGGCTACAATGGTACTATA
	Mm_Cenpe_3	AAGCATTGGGCTCGTGAATAA
	Mm_Cenpe_6	CAGCAACTTCTTAGTACACAA
CLASP1+2	Mm_Claspl_2	ACCGAGAGCAGTGTACGGAAA
	Mm_Claspl_4	CAGGTTCGAGACGCAGCAATA
	Mm_Claspl_5	CTGGTATTGAATGTAACGGAA
	Mm_Claspl_2	AAGGAGGATGGTGACACAATA
	Mm_Claspl_3	CAGGAAGAGTTCTAACCACAA
	Mm_Claspl_4	AACGCCAAGCTTGAAGGTAAA
	Mm_Claspl_5	CTGGTATTGAATGTAACGGAA
RACGAP1/CYK4	Mm_Racgap1_2	AAGATGGATATTGCCAATCTA
	Mm_Racgap1_3	CCGGATGGAGATTATCAATGA
	Mm_Racgap1_4	CTGGAGAAATTCAAAGACCTA
DLG5/HURP	Mm_Dlgap5_1	AGCAAGGATTGGAGTCGCTAA
	Mm_Dlgap5_2	CCCGAACAGTGTCCATCCACTA
	Mm_Dlg7_3	CTGGACGGATTACAAGATCAA
	Mm_Dlg7_4	ATGGATTGTTTCTCTGTTGAA
HAUS6	Mm_6230416J20Rik_1	TTGAGTGGTATTGGTATATTA
	Mm_6230416J20Rik_2	CAGAGTGATGTTGATGGGATA
	Mm_6230416J20Rik_3	CCAGAATTAGATTCTAATTTA
	Mm_6230416J20Rik_4	TAGACTGAGAATTTAATTCTA
KIF2A	Mm_Kif2a_2	AAGGAGTGCATCCGAGCCTTA
	Mm_Kif2a_3	CTGCTGGACCATTCCATCTTA
	Mm_Kif2a_5	CAGGATGTTGATGCTACAAAT
	Mm_Kif2a_7	CAGGAATGGCATCCTGTGAAA
KIF4A	Mm_Kif4_2	AAGAATTGGCTTGGAATGAA
	Mm_Kif4_3	TACGATGAAATACATGGTCAA
	Mm_Kif4_4	CAGGAAGTGGAGGGTCAAATA
KIF11/EG5	Mm_Kif11_2	AGCAAAGAACATAATGAATAA
	Mm_Kif11_3	CACAGGAACCTTGCCAGTTAA
	Mm_Kif11_4	TTCCATCTTGAACATAAATAA
KIF12	Mm_Kif12_2	AAGGCATATTAGAAAGGGAAA
	Mm_Kif12_3	AAGGCCTCTCTTCTTGTTAAA
	Mm_Kif12_4	AACCTGAGTCTCGGTTACAA
KIF14	Mm_Kif14_4	CTGGCTGGAAGTGGGAAATAA
	Mm_Kif14_7	ATGGATTAAGTTTATGTGAAA
	Mm_Kif14_8	TCGGCTTGAGGCAGAAATTAA
	Mm_Kif14_9	AAGCAGCATCTTGAACAGGAA
KIF15/HKLP2	Mm_Knsl7_1	AGGCTGGATAATGATATATTA

	Mm_Knsl7_2	CAGGATTCCTACGATAACTTA
	Mm_Knsl7_3	CACAATAGAATCAATGGAGAA
	Mm_Knsl7_4	CACATGGTAGAACTAAACTAA
KIF18A	Mm_Kif18a_2	TGCATTGTAAATATTGTTTAA
	Mm_Kif18a_3	CAGATTTATTTGCGACAACAA
	Mm_Kif18a_4	TTGGAGGAAACTGTCAAACATA
KIF20A/MLKP2	Mm_Kif20a_1	CAGGAAGTTAAAGCTGAACTA
	Mm_Kif20a_2	CAGCTAGATGAAACAAGTCAA
	Mm_Kif20a_3	CTCCTTTGCCTTGAAGAGTAA
	Mm_Kif20a_4	AACGGCAATCCTTACGTGAAA
KIF20B/MPP1	Mm_Mphospho1_1	AAGGAGGAAAGTGCTAACAAA
	Mm_Mphospho1_2	CAGGACTTAGATATGAAACAA
	Mm_Mphospho1_3	ACGGTAGAAGTAAGTAAAGAA
	Mm_Mphospho1_4	CAGATAGAAGATTCTGAAATA
KIF23/MKLP1	Mm_Kif23_1	AAGGCTGAAGACTATGAAGAA
	Mm_Kif23_2	TTGTTTGAATATGATCTTTAA
	Mm_Kif23_3	TACGATCTATGAGGAAGATAA
	Mm_Kif23_4	CTGAGTCATCTTGCAGAAGAA
KIFC1/HSET	Mm_LOC100502766_1	TACACTGGGACTGGTCATAAT
	Mm_LOC100502766_2	GTGAACAATATTTATTATGTA
	Mm_LOC100502766_3	CAGAGCCTGATTCCCTTGCAA
	Mm_LOC100502766_4	CTGCGCGGAGGTTGAAATTCA
KIFC2	Mm_Kifc2_2	CAGGCATTTGAGAGAGGGCAA
	Mm_Kifc2_3	CAGTGTCTGCATCTTCACTTA
	Mm_Kifc2_4	CAGTATGGTGGAGATCTACAA
KIFC3	Mm_Kifc3_2	CCGCACCACCGAGTTCACCAA
	Mm_Kifc3_3	CAGAGGTCTGGGCTATATTTA
	Mm_Kifc3_7	GGGCATGTATATAATGTTCTA
NUMA	Mm_Numa1_1	CAGGATAAGAAATGTCTTGAA
	Mm_Numa1_2	CAGCTGGACACTCTAAAGCAA
	Mm_Numa1_3	AATGTTATTACTTGTAATAA
	Mm_Numa1_4	CTGGAAGTAGAACTAGATCAA
PCNT	Mm_Pcnt2_2	AAGGAGATCCATGCAAAGCAA
	Mm_Pcnt2_3	CCGCCAGATTCTACTCAGAAA
	Mm_Pcnt2_4	TGGGATGTAATTGATATTATT
PRC1	Mm_Prc1_1	AAGGCTAGTTATGATAGTTAA
	Mm_Prc1_2	CTGGAGAACATTGCAACATTA
	Mm_Prc1_3	TCCGGGAAATATGGGAACTAA
	Mm_Prc1_4	CTGGATAGAATGATTGCTGAA
TPX2	Mm_Tpx2_1	CACGGGAACTTGATCCTAGAA
	Mm_Tpx2_2	CAAGGCAAATCCAATACGGAA
	Mm_Tpx2_5	CAGAGGATGCACTATCATTA
	Mm_Tpx2_8	CAGGTTGAAGCCTTCCACAAA